Inorganic Chemistry
Cite This: Inorg. Chem. XXXX, XXX, XXX−XXX
Article
pubs.acs.org/IC

Two-Photon Excited FRET Dyads for Lysosome-Targeted Imaging and Photodynamic Therapy

Mengliang Zhu,[†] Jinghui Zhang,[†] Yabin Zhou,[‡] Peipei Xing,[†,§] Lei Gong,[†] Chaorui Su,[†] Dongdong Qi,[†] Hongwu Du,[‡] Yongzhong Bian,*[,†] and Jianzhuang Jiang*[,†]

[†]Beijing Key Laboratory for Science and Application of Functional Molecular and Crystalline Materials, Department of Chemistry, University of Science and Technology Beijing, Beijing 100083, China

[‡]Department of Biology, University of Science and Technology Beijing, Beijing 100083, China

[§]Beijing Vocational College of Agriculture (Beiyuan), Beijing 100012, China

Supporting Information

ABSTRACT: Two-photon excitable fluorescent dyes with integrated functions of targeted imaging and photodynamic therapy (PDT) are highly desired for the development of cancer theranostic agents. Herein, fluorescence resonance energy transfer (FRET) dyads, AceDAN-H_2Por-Lyso (**1a**) and AceDAN-ZnPor-Lyso (**1b**), were developed for two-photon excited (TPE) lysosome-targeted fluorescence imaging and PDT of cancer cells. Under one-photon or two-photon excitation, the AceDAN donor can effectively transfer the excited state energy to the porphyrin acceptor via high efficient FRET, leading to the generation of deep-red fluorescence and singlet oxygen for cell imaging and PDT, respectively. **1a** and **1b** exhibit high photocytotoxicity and low dark cytotoxicity, in addition to strong lysosomal targeting capability in living cells. By taking the advantages of the two-photon absorption properties of the AceDAN donor and the properly distributed S_1 and T_1 states of the porphyrin acceptor, the AceDAN-porphyrin dyads **1a** and **1b** have been successfully applied to TPE-fluorescence imaging for tracking the significant morphology changes of cancer cells under two-photon laser irradiation.

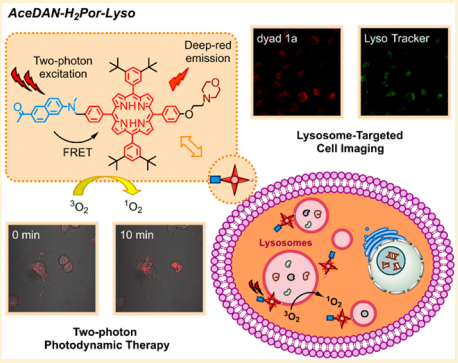

INTRODUCTION

Fluorescence imaging is a prominent detection technique for biomedical research due to the high-resolution, real-time, and nondestructive features.[1] The precise diagnosis and fluorescence-guided treatment of disease are pursued by applying analyte-specific and stimuli-responsive fluorescent probes to bioimaging.[2] In this respect, one encouraging strategy is to integrate the fluorescence imaging and the photodynamic therapy (PDT) modalities to formulate theranostic agents for the direct visualization and synchronized treatment of tumors.[3,4] However, most of the current fluorophores for theranostic agents are based on one-photon excitation (OPE) by ultraviolet−visible (UV−vis) light, which may suffer from low penetration depth and high background noise.[5] Alternatively, two-photon excitation (TPE)-based fluorophores allow for excitation with near-infrared (NIR) light,[6,7] which are feasible for achieving the advantages of deep tissue penetration, high spatial resolution, low background signal, and minimized side effects for TPE-fluorescence imaging[8] and TPE-PDT.[9] Nevertheless, conventional TPE dyes mostly emit in a relatively short and fixed spectral range of blue to green color (400−550 nm),[8] which may also restrict the clinical translation of TPE-fluorescence imaging. One of the goals of the current research is to develop TPE dyes with near-infrared (NIR) light emission characteristics.[10,11] An attractive approach for regulating the emission wavelength is to incorporate a TPE dye into a fluorescence resonance energy transfer (FRET) system as the energy donor.[12] Then, by choosing a proper FRET acceptor, the intrinsic emission of a TPE dye could be translated to the emission of the acceptor with a tunable manner.[13]

On the other hand, porphyrins have shown great potential in fluorescence imaging and PDT treatment of tumors[14,15] due to the superior photophysical properties and well established synthetic chemistry.[16] In particular, metal-free-[17] and some metallo-porphyrins[18] possess bright deep-red emissions from singlet excited states (S_1) due to the high extinction coefficients in the vis−NIR region and the substantial fluorescence quantum yields, which are desired for bioimaging applications. Furthermore, these porphyrins also have long-lived triplet excited states (T_1),[19] which are essential for the type-II PDT photosensitizers to generate singlet oxygen ($^1O_2$).[20,21] Together, porphyrin derivatives could simultaneously perform the dual functions of imaging agents and PDT photosensitizers by properly manipulating and distributing the S_1 and T_1 states.[22]

Received: June 7, 2018

DOI: 10.1021/acs.inorgchem.8b01581
Inorg. Chem. XXXX, XXX, XXX−XXX

Nevertheless, the cellular uptake efficacy and subcellular localization should be considered as well for the development of effective imaging and PDT agents.[23] Due to the short lifetime of singlet oxygen ($^1O_2$), the PDT outcome strongly depends on the subcellular localization of photosensitizers,[24] and organelle-targeted photosensitizers can specifically accumulate and efficiently induce apoptosis of cancer cells.[25,26] The lysosome, the recycling center of cells, is a kind of vesicle structure containing numerous hydrolases.[27] Singlet oxygen generated by activating lysosomal targeting photosensitizers can induce lysosomal damage and release hydrolytic enzymes into the cytoplasm, thereby leading to cell necrosis.[15,28]

On the basis of the above wisdom, herein we present the design of new functional porphyrins for two-photon excited lysosome-targeted fluorescence imaging and PDT. A two-photon absorption (TPA) donor and a lysosome-targeted moiety were attached to a porphyrin acceptor forming the new theranostic agents AceDAN-H_2Por-Lyso (**1a**) and AceDAN-ZnPor-Lyso (**1b**; Scheme 1). Upon two-photon excitation (TPE) with NIR light (740 nm), the donor could effectively transfer the excited state energy to the porphyrin acceptor via FRET. Then deep-red fluorescence (600−750 nm) and singlet oxygen ($^1O_2$) were generated from the porphyrin acceptor, which were utilized successfully for lysosome-targeted imaging and PDT of cancer cells.

Scheme 1. Structures of AceDAN-H_2Por-Lyso (1a); AceDAN-ZnPor-Lyso (1b); and the Reference Compounds AceDAN (2), H_2Por-Lyso (3a), and ZnPor-Lyso (3b)

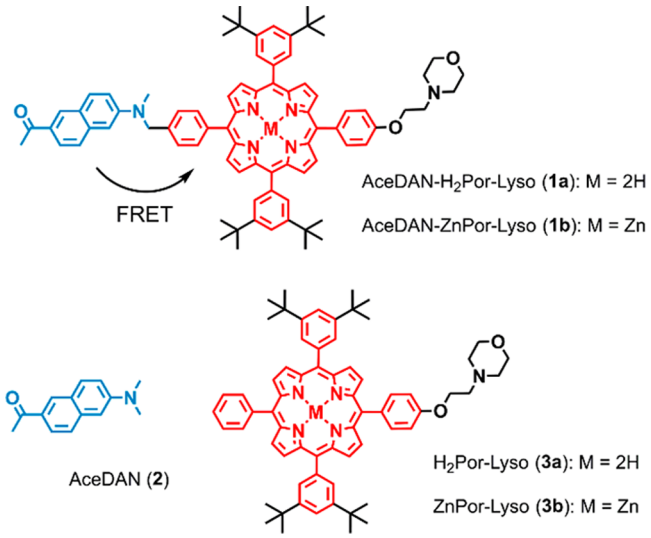

RESULTS AND DISCUSSION

Design and Synthesis. 2-Acetyl-6-dimethylaminonaphthalene (AceDAN),[29] as a typical TPE chromophore, was selected to pair up with a metal-free or zinc porphyrin (H_2Por or ZnPor) to formulate the FRET dyads. A morpholine (MPL) moiety was also incorporated into the TPE-FRET system for lysosome-targeted cell imaging[30] and to improve the PDT efficiency by lysosomal photodamage induced cell death.[31] The introduction of 3,5-di-*tert*-butylphenyl groups at the remaining *meso*-sites was expected to suppress the tendency of aggregation; thus it could increase the solubility and be beneficial for the fluorescent emission and singlet oxygen generation.

The lysosome-targeted dyads AceDAN-H_2Por-Lyso (**1a**) and AceDAN-ZnPor-Lyso (**1b**) were constructed from 5,15-diaryl-porphyrin precursors (**4a** and **4b**) via Suzuki−Miyaura coupling reactions[32] with phenylboronic acid ester derivatives of MPL and AceDAN successively (Scheme S1). The reference compounds H_2Por-Lyso (**3a**) and ZnPor-Lyso (**3b**) were synthesized by a similar procedure. The reference compound **2** was obtained by the methylation of **7** with methyl iodide (Scheme S2). All of the new compounds were sufficiently characterized by ^{1}H NMR, ^{1}H−^{1}H COSY, ^{13}C NMR, and ^{13}C−^{1}H COSY spectroscopies and mass spectrometry and elemental analysis (Figures S1−S9, Supporting Information).

Photophysical Properties. The photophysical data of AceDAN-H_2Por-Lyso (**1a**), AceDAN-ZnPor-Lyso (**1b**), and the reference compounds **2**, H_2Por-Lyso (**3a**) and ZnPor-Lyso (**3b**), are summarized in Table S1, Supporting Information. The ground state absorption spectra of **1a** and **1b** show the characteristic Soret bands (ca. 420 nm) and Q bands (500−650 nm) of porphyrins in addition to a less intense and broad absorption band of the AceDAN moiety centered at 370 nm (Figure 1a), which resembles the linear superimposition of those of compounds **3a** or **3b** with **2**, respectively, indicating

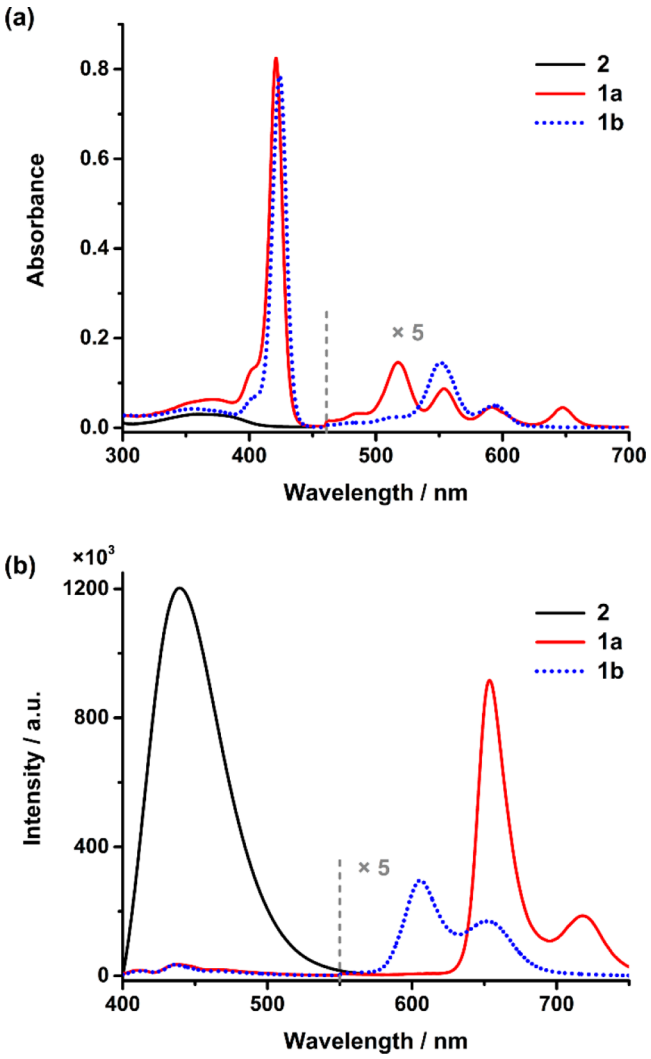

Figure 1. Absorption (a) and emission spectra (b) of AceDAN-H_2Por-Lyso (**1a**), AceDAN-ZnPor-Lyso (**1b**), and **2** in $CHCl_3$ (2 μM) with excitation at 370 nm.

DOI: 10.1021/acs.inorgchem.8b01581
Inorg. Chem. XXXX, XXX, XXX−XXX

the absence of strong electronic interactions between the porphyrin and AceDAN units in the ground state (Figure S10, Supporting Information).

Upon excitation at 370 nm, where the AceDAN moiety absorbs most of the light, **1a** and **1b** give the characteristic emissions of H_2Por (λ_{max} = 654 nm, τ = 7.78 ns, Φ_{em} = 0.14) and ZnPor (λ_{max} = 606 nm, τ = 1.62 ns, Φ_{em} = 0.036), respectively, and a very weak emission band of AceDAN (λ_{max} = 436−438 nm, Φ_{em} = 0.011−0.013; Figures 1b and S11, Supporting Information). As expected, the AceDAN emissions of **1a** and **1b** are significantly quenched in comparison with that of the reference **2** (λ_{max} = 440 nm, Φ_{em} = 0.49), while the emissions of H_2Por and ZnPor are obviously enhanced relative to those of **3a** and **3b** under the same experimental conditions (Figure S12, Supporting Information). This observation indicates the occurrence of intramolecular FRET from the AceDAN donor to the porphyrin acceptor, which is further supported by comparing the excitation spectra of **1a** and **1b** with those of **3a** and **3b** in the range of 300−400 nm (where the absorption of the AceDAN moiety dominates, Figure S12 in the Supporting Information). The efficiencies of energy transfer (η_{EET}) were estimated to be up to 97% for **1a** and 98% for **1b**,[18] which are believed to be due to the effective spectral overlaps between the AceDAN emission and the porphyrin absorption as well as the short distance between the two fluorophores (Figures S13 and S14, Supporting Information).[33]

The two-photon absorption cross section (δ_{TPA}) values of **1a**, **1b**, and **2** in the range of 720−880 nm were determined by using the two-photon excited fluorescence measurement technique.[6] The peak δ_{TPA} values of **1a** (112 GM) and **1b** (95 GM) are obtained at 740 nm (Figure 2a), which are obviously inherited from the AceDAN moiety, as the reference compound **2** (120 GM) exhibits a larger δ_{TPA} value than **3a** (25 GM) and **3b** (12 GM) at this wavelength.[8] Under the optimum two-photon excitation at 740 nm with femtosecond pulses, compound **2** exhibits a strong fluorescence emission peak at 440 nm, which is translated to the characteristic emissions of porphyrin in the deep-red region (Figure 2b). In addition, **1a** and **1b** show enhanced two-photon fluorescence emission responses in comparison with **3a** and **3b** under the same excitation conditions (Figure S15, Supporting Information). These results confirm that the two-photon absorption of the AceDAN donor could be utilized to efficiently generate the excited states of the porphyrin acceptor via FRET, thus indicating the high potential in TPE-fluorescence imaging and TPE-PDT.

Lysosome-Targeted Cell Imaging under One-Photon Excitation. The cell imaging performance was first evaluated under one-photon excitation by confocal laser scanning microscopy (CLSM). To verify the lysosome-targeting ability, a commercial lysosome-targeting dye, LysoTracker Green DND-26, was applied to costain A549 cells with **1a** and **1b**, respectively. The A549 cells were incubated with **1a** or **1b** (8 μM in DMEM, with 0.4% DMSO and 0.1% Cremophor EL,[34] v/v) at 37 °C for 15 min and then incubated with LysoTracker Green DND-26 (100 nM) for another 5 min. As shown in Figure 3, the red fluorescence from **1a** and **1b** overlapped well with the green fluorescence from DND-26. The Pearson's coefficients[35] of the red channel and green channel were calculated to be 0.81 and 0.86 for **1a** and **1b**, respectively. And the overlap coefficients were 0.85 and 0.89 for **1a** and **1b**, respectively (Figure S16, Supporting Information). Moreover,

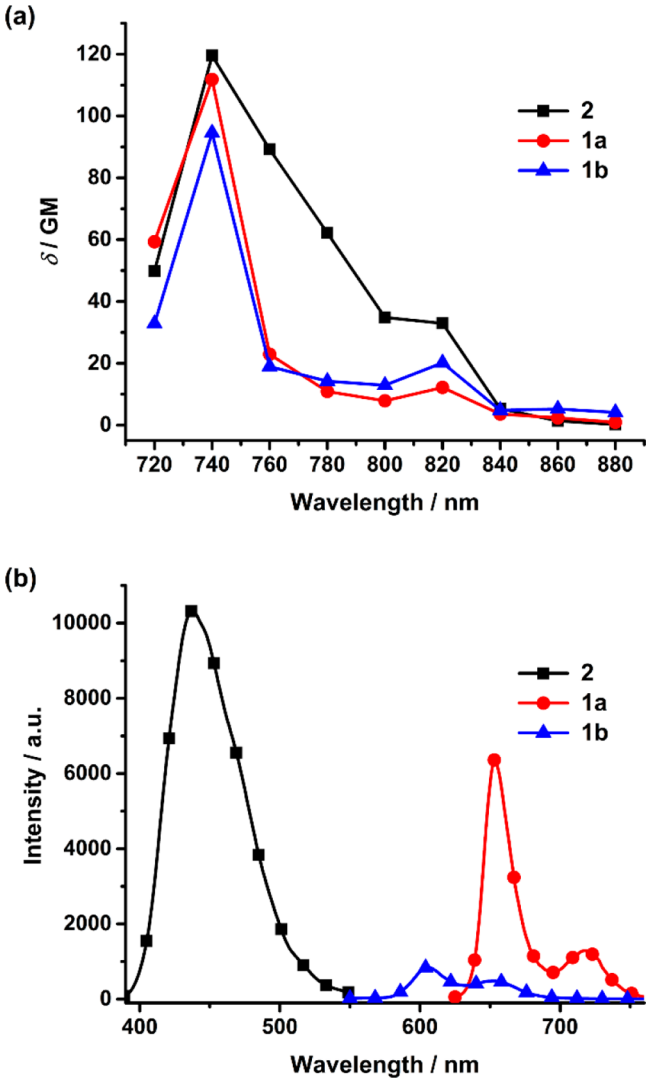

Figure 2. Two-photon absorption cross section (a) and two-photon excited emission spectra (b) of AceDAN-H_2Por-Lyso (**1a**), AceDAN-ZnPor-Lyso (**1b**), and **2** in $CHCl_3$ (5 μM) with two-photon excitation at 740 nm with 100 fs pulses.

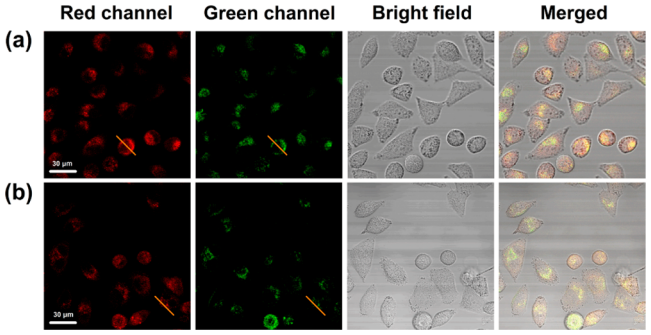

Figure 3. (a) Colocalization images of A549 cells stained with **1a** (8 μM, red channel, λ_{ex} = 405 nm, λ_{em} = 550−750 nm) and DND-26 (100 nM, green channel, λ_{ex} = 488 nm, λ_{em} = 500−550 nm). (b) Colocalization images of A549 cells stained with **1b** (8 μM, red channel, λ_{ex} = 405 nm, λ_{em} = 550−750 nm) and DND-26 (100 nM, green channel, λ_{ex} = 488 nm, λ_{em} = 500−550 nm). The orange lines in the red and green channels represent the region of interest (ROI) across the A549 cells.

DOI: 10.1021/acs.inorgchem.8b01581
Inorg. Chem. XXXX, XXX, XXX−XXX

the variations of intensity profiles in the linear region of interest (ROI; given by orange lines in Figure 3) are almost synchronous in the two channels (Figure S17, Supporting Information). These observations indicate that **1a** and **1b** are colocalized with the commercial LysoTracker, thus confirming the specific lysosomal targeting in living cells.

Singlet Oxygen Generation and Photocytotoxicity under One-Photon Excitation. To evaluate the potential as effective photosensitizers for PDT, the singlet oxygen generation of **1a** and **1b** under one-photon excitation was first performed using a chemical trapping method[36] with 1,3-diphenylisobenzofuran (DPBF) as an efficient $^1O_2$ scavenger.[37] From the time-dependent absorption changes of DPBF (Figure S18, Supporting Information), it is clear that the presence of **1a** and **1b** leads to the fast decay of DPBF upon yellow light (λ > 490 nm) irradiation, while **1a** induces a higher decay rate of DPBF than that of **1b**, indicating a higher $^1O_2$ generation efficiency of the former. The quantum yields of $^1O_2$ production (Φ_Δ) were then determined by measuring the NIR phosphorescence of $^1O_2$ (ca. 1275 nm)[38] upon excitation at 370 nm. Distinct emissions around 1275 nm were observed in the presence of **1a** and **1b**, Figure 4a. The integral intensities of $^1O_2$ emissions are linearly proportion to the optical density (OD = 0.01−0.05) values of the utilized photosensitizers, Figure 4b. Thus, by reference to tetraphenylporphyrin (TPP, Φ_Δ = 0.55),[39] the $^1O_2$ quantum yields were obtained for **1a** (0.57) and **1b** (0.66), respectively. The substantial $^1O_2$ generation of **1a** and **1b** is believed to be mainly based on the intramolecular FRET from the excited AceDAN donor to the porphyrin acceptor;[40] thereafter, the intersystem crossing (ISC) of the excited porphyrin moiety and the intermolecular triplet−triplet energy transfer to the ground state of $^3O_2$ are involved.[14] In addition, it is noted that **1b** showed a higher Φ_Δ value than **1a**, which can be attributed to the different distribution of S_1 and T_1 states between H_2Por and ZnPor.[22]

The cytotoxicities of **1a** and **1b** (1−8 μM) were examined on A549 cells in the dark and under light irradiation (λ_{ex} > 490 nm, 18 J·cm^{-2}), respectively. As shown in Figure 5, **1a** and **1b** were essentially noncytotoxic to A549 cells (viability > 90% at 8 μM) in the absence of light, but displayed significant photocytotoxicity with increasing concentration from 1 to 8 μM. According to the survival curves in the presence of light, the impressive photocytotoxicity with IC_{50} values of 3.1 and 4.6 μM were obtained for **1a** and **1b**, respectively.

Two-Photon Excited Cell Imaging and PDT. TPE-fluorescence imaging of **1a** and **1b** toward A549 cells was performed under the irradiation of a 740 nm femtosecond laser (115 mW, 80 MHz, 140 fs) by CLSM. The morphology changes of cells were tracked within 0−30 min to access the TPE-PDT feasibility (Figure 6). Both **1a** and **1b** could get into A549 cells after 15 min of incubation and show strong red fluorescence under two-photon excitation. The images of two-photon (TP) mode are coincident with those of one-photon (OP) mode and bright field, indicating the promising TPE-fluorescence imaging performance of **1a** and **1b**.

After a 740 nm laser scan for 10 min, the fluorescence of **1a** and **1b** in A549 cells was diffused and enhanced, suggesting the disruption of lysosomes and other membrane structures in cytoplasm. As the irradiation time was prolonged, blebs were formed on the cell boundaries accompanied by obvious cell shrinkage, which may indicate the rupture of the cell membrane. After 30 min of laser scanning, A549 cells loaded with **1a** or **1b** had lost their morphological integrity or even

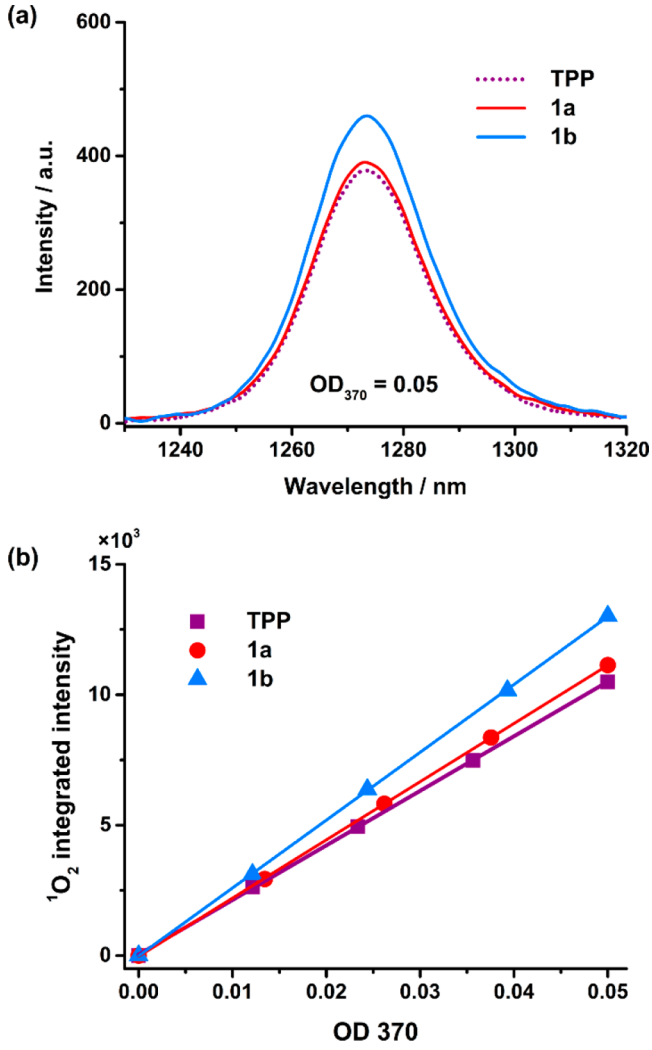

Figure 4. (a) The NIR phosphorescence emission spectra of singlet oxygen obtained from O_2-saturated solutions of **1a**, **1b**, and TPP (OD = 0.05) with excitation at 370 nm in $CHCl_3$. (b) The relative intensity of $^1O_2$ emission versus absorption at 370 nm.

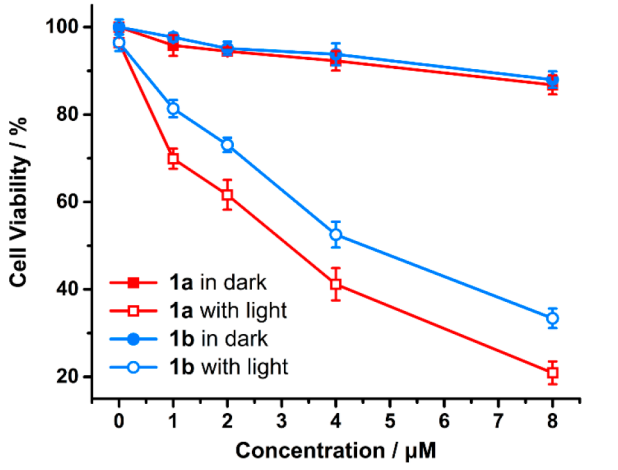

Figure 5. Dark and photocytotoxicity (λ_{ex} > 490 nm, light dose 18 J·cm^{-2}) of **1a** and **1b** (1−8 μM) on A549 cells obtained by a MTT assay.

obviously deformed, leaving only residues, which represents cell death. For comparison, the cells without photosensitizer

DOI: 10.1021/acs.inorgchem.8b01581
Inorg. Chem. XXXX, XXX, XXX−XXX

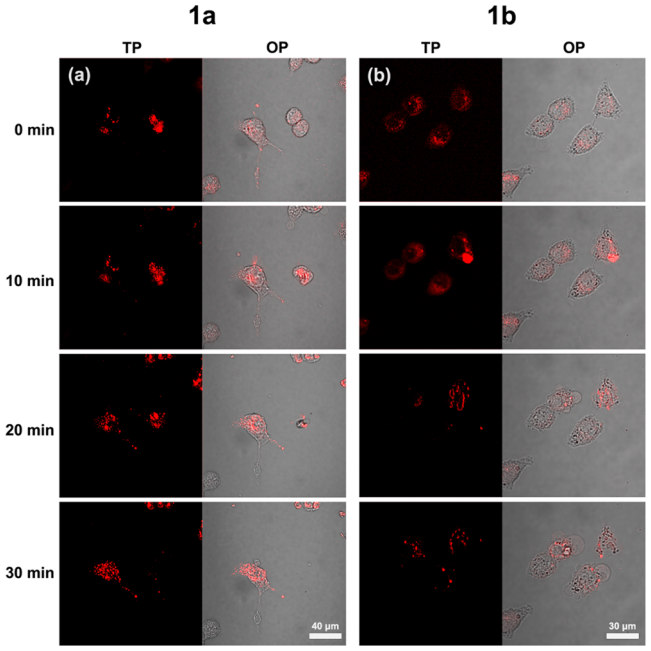

Figure 6. Two-photon (TP, red channel, λ_{ex} = 740 nm) and one-photon (OP, red channel, λ_{ex} = 405 nm, merged with bright field) confocal images of A549 cells treated with 8 μM of **1a** (a) and **1b** (b). Images were obtained after different times (0−30 min) of laser irradiation (740 nm, 115 mW, 80 MHz, 140 fs).

showed no significant change under the same irradiation (Figure S19, Supporting Information). These observations clearly demonstrate that **1a** and **1b** possess strong photocytotoxicity under two-photon excitation, thus they can hopefully be photosensitizers for TPE-PDT.

CONCLUSION

In summary, we have developed AceDAN-porphyrin dyads **1a** and **1b** for lysosome-targeted two-photon excited fluorescence imaging and PDT of cancer cells. Upon one-photon or two-photon excitation of the AceDAN donor, intramolecular FRET processes occurred with high energy transfer efficiencies (η_{EET} = 97−98%), leading to the formation of the excited porphyrin acceptor, from which deep-red fluorescence (600−750 nm) and singlet oxygen were generated and utilized for cell imaging and PDT simultaneously. **1a** and **1b** exhibited strong lysosome-targeting abilities and low cytotoxicity in the dark, while displaying high photocytotoxicity with IC_{50} values as low as 3.1 and 4.6 μM under irradiation (λ_{ex} > 490 nm, 18 J·cm^{-2}). The AceDAN-porphyrin dyads were also successfully used in TPE-fluorescence imaging for tracking the significant morphology changes of A549 cells under the irradiation of a 740 nm femtosecond laser, thus demonstrating a promising TPE-FRET strategy for the development of cancer theranosis.

EXPERIMENTAL SECTION

Synthesis and Characterization of 1a and 1b. *5,15-Bis[3,5-di(tert-butyl)phenyl]-10-[4-(2-morpholinoethoxy)phenyl]-20-[4-[[(6-acetyl-2-naphthalenyl)methylamino]methyl]phenyl]porphyrin (**1a**).* To a solution containing compound **6a** (48.5 mg, 0.05 mmol) in toluene (10 mL) were added Cs_2CO_3 (82 mg, 0.25 mmol), $Pd(PPh_3)_4$ (12 mg, 0.01 mmol), and compound **8** (22.8 mg, 0.055 mmol, 1.1 equiv). The resulting reaction mixture was refluxed for 15 h under N_2 and then cooled to room temperature. The solvent was removed under reduced pressure. The residue was chromatographed on a silica gel column (CH_2Cl_2/C_2H_5OH = 100:2), where the first fraction was collected and evaporated. Repeated chromatography ($CHCl_3$) followed by recrystallization from $CHCl_3$ and ethanol gave pure target compound as a purple powder (20 mg, 34%). ^{1}H NMR ($CDCl_3$, 400 MHz, 293 K): δ 8.87 (d, J = 4.0 Hz, 6H), 8.84 (d, J = 4.0 Hz, 2H), 8.38 (s, 1H), 8.19 (d, J = 8.0 Hz, 2H), 8.13 (d, J = 8.0 Hz, 2H), 8.09 (s, 4H), 7.98 (d, J = 8.0 Hz, 1H), 7.92 (d, J = 12.0 Hz, 1H), 7.80 (s, 2H), 7.73 (d, J = 8.0 Hz, 1H), 7.62 (d, J = 8.0 Hz, 2H), 7.43 (dd, J = 8.0 Hz, J = 4.0 Hz, 1H), 7.28 (d, J = 8.0 Hz, 2H), 7.15 (s, 1H), 5.05 (s, 2H), 4.41 (t, J = 4.0 Hz, 2H), 3.84 (t, J = 4.0 Hz, 4H), 3.43 (s, 3H), 3.01 (t, J = 4.0 Hz, 2H), 2.73 (t, J = 4.0 Hz, 4H), 2.70 (s, 3H), 1.53 (s, 36H), −2.71 (s, 2H). ^{13}C NMR ($CDCl_3$, 100 MHz, 293 K): δ 197.9, 158.7, 149.9, 148.9, 141.4, 138.0, 137.7, 135.7, 135.1, 131.2, 130.5, 130.1, 126.5, 125.5, 125.1, 124.9, 121.6, 121.2, 116.6, 113.0, 105.8, 67.2, 66.4, 58.1, 56.7, 54.4, 39.2, 35.2, 31.9, 26.6. MALDI-TOF-MS, m/z calcd for $C_{80}H_{86}N_6O_3$ (M^+): 1178.7. Found: 1178.8. Anal. calcd for $C_{80}H_{86}N_6O_3$: C, 81.46; H, 7.35; N, 7.12. Found: C, 81.23; H, 7.39; N, 7.15.

*5,15-Bis[3,5-di(tert-butyl)phenyl]-10-[4-(2-morpholinoethoxy)-phenyl]-20-[4-[[(6-acetyl-2-naphthalenyl)methylamino]methyl]-phenyl]porphyrinatozinc (**1b**).* By using the procedure described above with **6b** (52 mg, 0.05 mmol) instead of **6a** as the starting material, **1b** was obtained as a reddish purple powder (31 mg, 50%). ^{1}H NMR ($CDCl_3$, 400 MHz, 293 K): δ 8.89−8.95 (m, 8H), 8.35 (s, 1H), 8.18 (d, J = 8.0 Hz, 2H), 8.10 (d, J = 8.0 Hz, 2H), 8.07 (s, 4H), 7.95 (d, J = 8.0 Hz, 1H), 7.89 (d, J = 8.0 Hz, 1H), 7.78 (s, 2H), 7.71 (d, J = 8.0 Hz, 1H), 7.59 (d, J = 8.0 Hz, 2H), 7.41 (d, J = 8.0 Hz, 1H), 7.22 (d, J = 8.0 Hz, 2H), 7.13 (s, 1H), 5.04 (s, 2H), 4.30 (s, 2H), 3.47 (s, 4H), 3.41 (s, 3H), 2.87 (s, 2H), 2.67 (s, 3H), 2.46 (s, 4H), 1.53 (s, 36H). ^{13}C NMR ($CDCl_3$, 100 MHz, 293 K): δ 197.9, 158.4, 150.0, 148.5, 142.6, 142.3, 138.0, 137.2, 135.5, 135.0, 131.2, 131.1, 130.5, 130.0, 126.4, 125.5, 124.9, 124.8, 122.5, 122.4, 120.7, 116.6, 112.7, 105.7, 66.8, 66.1, 57.9, 56.7, 54.0, 39.2, 35.2, 31.9, 26.6. MALDI-TOF-MS, m/z calcd for $C_{80}H_{84}N_6O_3Zn$ (M^+): 1240.6. Found: 1241.1. Anal. calcd for $C_{80}H_{84}N_6O_3Zn$: C, 77.31; H, 6.81; N, 6.76. Found: C, 77.83; H, 6.76; N, 6.71.

ASSOCIATED CONTENT

Supporting Information

The Supporting Information is available free of charge on the ACS Publications website at DOI: 10.1021/acs.inorgchem.8b01581.

Chemicals and instruments, measurement of the photophysical properties, dark and photocytotoxicity assay, cell culture and confocal microscopy studies, synthesis and characterization details, DFT calculation of dyad **1b**, Schemes S1 and S2, Figures S1−S19, and Table S1 (PDF)

AUTHOR INFORMATION

Corresponding Authors

*E-mail: yzbian@ustb.edu.cn.
*E-mail: jianzhuang@ustb.edu.cn.

ORCID

Yongzhong Bian: 0000-0003-0621-3683
Jianzhuang Jiang: 0000-0002-4263-9211

Notes

The authors declare no competing financial interest.

ACKNOWLEDGMENTS

Financial support from the National Natural Science Foundation of China (21471015, 21631003 and 21671017), Beijing Natural Science Foundation, and Fundamental Research Funds for the Central Universities is gratefully acknowledged.

DOI: 10.1021/acs.inorgchem.8b01581
Inorg. Chem. XXXX, XXX, XXX−XXX

REFERENCES

(1) Chen, X.; Lee, K.; Ren, X.; Ryu, J.; Kim, G.; Ryu, J.; Lee, W.; Yoon, J. Synthesis of a Highly HOCl-Selective Fluorescent Probe and Its Use for Imaging HOCl in Cells and Organisms. *Nat. Protoc.* **2016**, *11*, 1219−1228.

(2) Antaris, A. L.; Chen, H.; Cheng, K.; Sun, Y.; Hong, G.; Qu, C.; Diao, S.; Deng, Z.; Hu, X.; Zhang, B.; Zhang, X.; Yaghi, O. K.; Alamparambil, Z. R.; Hong, X.; Cheng, Z.; Dai, H. A Small-Molecule Dye for NIR-II Imaging. *Nat. Mater.* **2016**, *15*, 235−242.

(3) Celli, J. P.; Spring, B. Q.; Rizvi, I.; Evans, C. L.; Samkoe, K. S.; Verma, S.; Pogue, B. W.; Hasan, T. Imaging and Photodynamic Therapy: Mechanisms, Monitoring, and Optimization. *Chem. Rev.* **2010**, *110*, 2795−2838.

(4) Gao, M.; Yu, F.; Lv, C.; Choo, J.; Chen, L. Fluorescent Chemical Probes for Accurate Tumor Diagnosis and Targeting Therapy. *Chem. Soc. Rev.* **2017**, *46*, 2237−2271.

(5) Ai, X.; Mu, J.; Xing, B. Recent Advances of Light-Mediated Theranostics. *Theranostics* **2016**, *6*, 2439−2457.

(6) Pawlicki, M.; Collins, H. A.; Denning, R. G.; Anderson, H. L. Two-Photon Absorption and the Design of Two-Photon Dyes. *Angew. Chem., Int. Ed.* **2009**, *48*, 3244−3266.

(7) He, G. S.; Tan, L.; Zheng, Q.; Prasad, P. N. Multiphoton Absorbing Materials: Molecular Designs, Characterizations, and Applications. *Chem. Rev.* **2008**, *108*, 1245−1330.

(8) Kim, H. M.; Cho, B. R. Small-Molecule Two-Photon Probes for Bioimaging Applications. *Chem. Rev.* **2015**, *115*, 5014−5055.

(9) Sun, Z.; Zhang, L.; Wu, F.; Zhao, Y. Photosensitizers for Two-Photon Excited Photodynamic Therapy. *Adv. Funct. Mater.* **2017**, *27*, 1704079.

(10) Pascal, S.; Denis-Quanquin, S.; Appaix, F.; Duperray, A.; Grichine, A.; Le Guennic, B.; Jacquemin, D.; Cuny, J.; Chi, S.; Perry, J. W.; van der Sanden, B.; Monnereau, C.; Andraud, C.; Maury, O. Keto-Polymethines: A Versatile Class of Dyes with Outstanding Spectroscopic Properties for in Cellulo and in Vivo Two-Photon Microscopy Imaging. *Chem. Sci.* **2017**, *8*, 381−394.

(11) Horton, N. G.; Wang, K.; Kobat, D.; Clark, C. G.; Wise, F. W.; Schaffer, C. B.; Xu, C. In Vivo Three-Photon Microscopy of Subcortical Structures within an Intact Mouse Brain. *Nat. Photonics* **2013**, *7*, 205−209.

(12) Brousmiche, D. W.; Serin, J. M.; Fréchet, J. M.; He, G. S.; Lin, T.; Chung, S. J.; Prasad, P. N. Fluorescence Resonance Energy Transfer in a Novel Two-Photon Absorbing System. *J. Am. Chem. Soc.* **2003**, *125*, 1448−1449.

(13) Yuan, L.; Jin, F.; Zeng, Z.; Liu, C.; Luo, S.; Wu, J. Engineering a FRET Strategy to Achieve a Ratiometric Two-Photon Fluorescence Response with a Large Emission Shift and Its Application to Fluorescence Imaging. *Chem. Sci.* **2015**, *6*, 2360−2365.

(14) Ethirajan, M.; Chen, Y.; Joshi, P.; Pandey, R. K. The Role of Porphyrin Chemistry in Tumor Imaging and Photodynamic Therapy. *Chem. Soc. Rev.* **2011**, *40*, 340−362.

(15) Josefsen, L. B.; Boyle, R. W. Unique Diagnostic and Therapeutic Roles of Porphyrins and Phthalocyanines in Photodynamic Therapy, Imaging and Theranostics. *Theranostics* **2012**, *2*, 916.

(16) Li, C.; Zhang, J.; Song, J.; Xie, Y.; Jiang, J. Synthetic Porphyrin Chemistry in China. *Sci. China: Chem.* **2018**, *61*, 511−514.

(17) Zhu, M.; Zhou, Y.; Yang, L.; Li, L.; Qi, D.; Bai, M.; Chen, Y.; Du, H.; Bian, Y. Synergistic Coupling of Fluorescent "Turn-Off" with Spectral Overlap Modulated FRET for Ratiometric Ag^{+} Sensor. *Inorg. Chem.* **2014**, *53*, 12186−12190.

(18) Zhang, D.; Zhu, M.; Zhao, L.; Zhang, J.; Wang, K.; Qi, D.; Zhou, Y.; Bian, Y.; Jiang, J. Ratiometric Fluorescent Detection of Pb^{2+} by FRET-Based Phthalocyanine-Porphyrin Dyads. *Inorg. Chem.* **2017**, *56*, 14533−14539.

(19) Lee, H.; Hong, K.; Jang, W. Design and Applications of Molecular Probes Containing Porphyrin Derivatives. *Coord. Chem. Rev.* **2018**, *354*, 46−73.

(20) Dichtel, W. R.; Serin, J. M.; Edder, C.; Fréchet, J. M.; Matuszewski, M.; Tan, L.; Ohulchanskyy, T. Y.; Prasad, P. N. Singlet Oxygen Generation via Two-Photon Excited FRET. *J. Am. Chem. Soc.* **2004**, *126*, 5380−5381.

(21) Ogilby, P. R. Singlet Oxygen: There is Indeed Something New Under the Sun. *Chem. Soc. Rev.* **2010**, *39*, 3181−3209.

(22) Singh, S.; Aggarwal, A.; Bhupathiraju, N. D. K.; Arianna, G.; Tiwari, K.; Drain, C. M. Glycosylated Porphyrins, Phthalocyanines, and Other Porphyrinoids for Diagnostics and Therapeutics. *Chem. Rev.* **2015**, *115*, 10261−10306.

(23) Lovell, J. F.; Liu, T. W. B.; Chen, J.; Zheng, G. Activatable Photosensitizers for Imaging and Therapy. *Chem. Rev.* **2010**, *110*, 2839−2857.

(24) Bolze, F.; Jenni, S.; Sour, A.; Heitz, V. Molecular Photosensitisers for Two-Photon Photodynamic Therapy. *Chem. Commun.* **2017**, *53*, 12857−12877.

(25) Rajendran, L.; Knölker, H.; Simons, K. Subcellular Targeting Strategies for Drug Design and Delivery. *Nat. Rev. Drug Discovery* **2010**, *9*, 29−42.

(26) Zhou, Z.; Song, J.; Nie, L.; Chen, X. Reactive Oxygen Species Generating Systems Meeting Challenges of Photodynamic Cancer Therapy. *Chem. Soc. Rev.* **2016**, *45*, 6597−6626.

(27) Zhu, H.; Fan, J.; Du, J.; Peng, X. Fluorescent Probes for Sensing and Imaging within Specific Cellular Organelles. *Acc. Chem. Res.* **2016**, *49*, 2115−2126.

(28) Huang, H.; Yu, B.; Zhang, P.; Huang, J.; Chen, Y.; Gasser, G.; Ji, L.; Chao, H. Highly Charged Ruthenium(II) Polypyridyl Complexes as Lysosome-Localized Photosensitizers for Two-Photon Photodynamic Therapy. *Angew. Chem., Int. Ed.* **2015**, *54*, 14049−14052.

(29) Kim, H. M.; An, M. J.; Hong, J. H.; Jeong, B. H.; Kwon, O.; Hyon, J.; Hong, S.; Lee, K. J.; Cho, B. R. Two-Photon Fluorescent Probes for Acidic Vesicles in Live Cells and Tissue. *Angew. Chem., Int. Ed.* **2008**, *47*, 2231−2234.

(30) Zhu, M.; Xing, P.; Zhou, Y.; Gong, L.; Zhang, J.; Qi, D.; Bian, Y.; Du, H.; Jiang, J. Lysosome-Targeting Ratiometric Fluorescent pH Probes Based On Long-Wavelength BODIPY. *J. Mater. Chem. B* **2018**, *6*, 4422−4426.

(31) Aits, S.; Jäättelä, M. Lysosomal Cell Death at a Glance. *J. Cell Sci.* **2013**, *126*, 1905−1912.

(32) Suzuki, A. Cross-Coupling Reactions of Organoboranes: An Easy Way to Construct C-C Bonds (Nobel Lecture). *Angew. Chem., Int. Ed.* **2011**, *50*, 6722−6737.

(33) According to preliminary DFT modeling, the distance of the AceDAN donor and the porphyrin acceptor have been adjusted to 10.68 Å, see the Supporting Information for details.

(34) Gelderblom, H.; Verweij, J.; Nooter, K.; Sparreboom, A. Cremophor EL: The Drawbacks and Advantages of Vehicle Selection for Drug Formulation. *Eur. J. Cancer* **2001**, *37*, 1590−1598.

(35) Here, the Pearson's correlation coefficient (PCC) is defined as the linear correlation between the fluorescent intensities from two images/channels, see: Manders, E. M. M.; Verbeek, F. J.; Aten, J. A. Measurement of Co-Localization of Objects in Dual-Colour Confocal Images. *J. Microsc.* **1993**, *169*, 375−382.

(36) Liu, J.; Chen, Y.; Li, G.; Zhang, P.; Jin, C.; Zeng, L.; Ji, L.; Chao, H. Ruthenium(Ii) Polypyridyl Complexes as Mitochondria-Targeted Two-Photon Photodynamic Anticancer Agents. *Biomaterials* **2015**, *56*, 140−153.

(37) Young, R. H.; Wehrly, K.; Martin, R. L. Solvent Effects in Dye-Sensitized Photooxidation Reactions. *J. Am. Chem. Soc.* **1971**, *93*, 5774−5779.

(38) Nosaka, Y.; Nosaka, A. Y. Generation and Detection of Reactive Oxygen Species in Photocatalysis. *Chem. Rev.* **2017**, *117*, 11302−11336.

(39) Schmidt, R.; Afshari, E. Comment on "Effect of Solvent on the Phosphorescence Rate Constant of Singlet Molecular Oxygen ($^1\Delta_g$)". *J. Phys. Chem.* **1990**, *94*, 4377−4378.

(40) The direct-excitation of the Por moiety may also contribute because the absorption of Por at 370 nm cannot be neglected.

DOI: 10.1021/acs.inorgchem.8b01581
Inorg. Chem. XXXX, XXX, XXX−XXX